Zuschriften

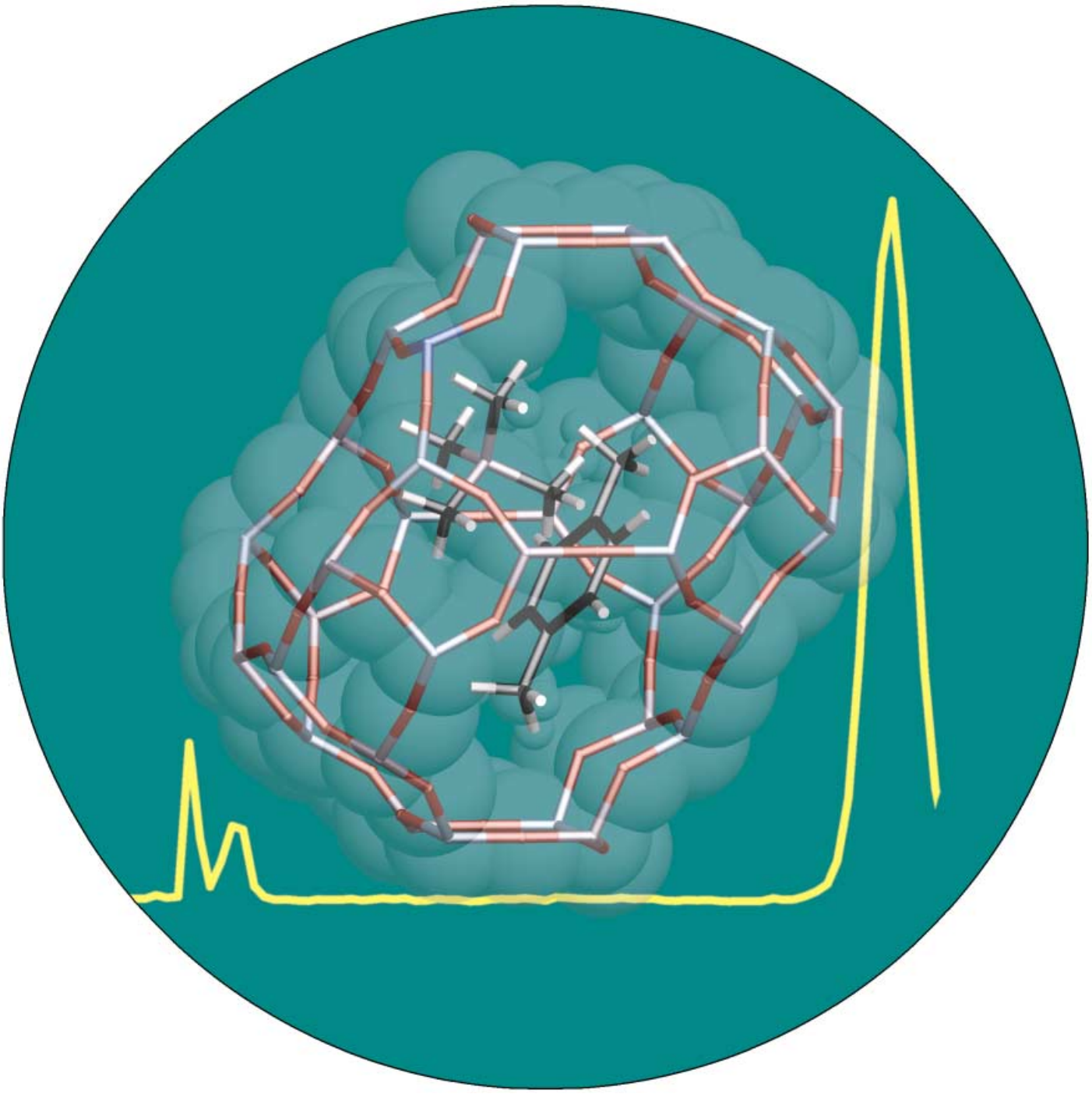

Die Synthese von Tetramethylphosphoniumkationen in den Hohlräumen von HSAPO-34 (hier abgebildet) durch einen Buddelschiff-Ansatz und die anschließende Calcinierung dieses Materials – hierbei entsteht ein aktiver Katalysator für die Umwandlung von Methanol in Alkene – wird von J. F. Haw und W. Song auf den folgenden Seiten beschrieben.

  0044-8249/03/11508-0919 $ 20.00+.50/0

Methanol-to-Olefin Catalyst

Improved Methanol-to-Olefin Catalyst with Nanocages Functionalized through Ship-in-a-Bottle Synthesis from PH_3**

*Weiguo Song and James F. Haw**

The catalytic conversion of methanol into olefins[1] is the remaining link in a chain of catalytic processes that convert natural gas into polyolefins. The most promising catalysts for commercial use are solid acids based on silico-aluminophosphates of the chabazite (CHA) structure, specifically HSAPO-34, which has one acid site per cage when prepared by our method.[2]. We recently demonstrated that the active site for methanol-to-olefin (MTO) chemistry on HSAPO-34 is a composite of an inorganic acid site and a methylbenzene molecule.[3] The latter self-assembles during a kinetic induction period and can not pass through the 0.38-nm windows interconnecting the 1.0 nm × 0.67 nm cages of the HSAPO-34 structure. The organic component is a scaffold on which carbon–carbon bonds can be formed and broken without recourse to high-energy intermediates and transition states. Herein, we build on this prior work to rationally design HSAPO-34 catalysts with improved selectivity, a very desirable property. Since we now know that MTO chemistry occurs in a nanometer-size cage already partially filled by a large hydrocarbon molecule, it is reasonable to say that olefin selectivity should be sensitive to further steric constraints.

For our first attempt at functionalization, we chose phosphorus chemistry, because phosphate species are hydrothermally stable modifiers of aluminosilicate zeolites,[4] and because we could use solid-state ^{31}P NMR spectroscopy to correlate structure with activity and selectivity. Few phosphorus reagents are adsorbed into HSAPO-34; $P(CH_3)_3$ is sterically excluded, and neither $PH(CH_3)_2$ nor PH_2CH_3 are commercially available. Thus, we chose PH_3, a toxic and pyrophoric gas that nevertheless proved to be easily handled by using lecture bottles and standard bench-top reactors assembled in a fume hood. Scheme 1 outlines our strategy for the modification of HSAPO-34 through ship-in-a-bottle routes starting with PH_3. In every case we held approximately 300 mg of HSAPO-34 in a flow reactor at 523 K and then introduced PH_3 gas into the He flow stream, while simultaneously delivering methanol by using a syringe pump. Each step in the scheme was achieved,[5] and representative ^{31}P spectra of thermally quenched catalyst beds are shown in Figure 1. In each spectrum, the ^{31}P resonance signal at $\delta = -28$ ppm arises from the phosphorus atoms in the framework. The initial products were protonated $P(CH_3)_3$ molecules ($\delta = -4$ ppm) and $P(CH_3)_4^+$ ions ($\delta = 23$ ppm).[6] The relative yields of these species are controlled by varying the ratio of PH_3 to CH_3OH. $P(CH_3)_3$ is commonly used as a spectroscopic probe for acidity.[7] The observation that all of the $P(CH_3)_3$ molecules in HSAPO-34 are protonated to $HP(CH_3)_3^+$ ions, and none is complexed to Lewis sites (Figure 1 a), is in itself an important finding. As Figure 1 c shows, we synthesized one

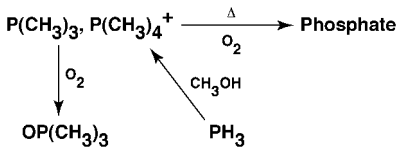

Scheme 1. Ship-in-a-bottle reactions of phosphane, methanol, and oxygen leading to a phosphate-modified HSAPO-34 catalyst with improved ethylene selectivity.

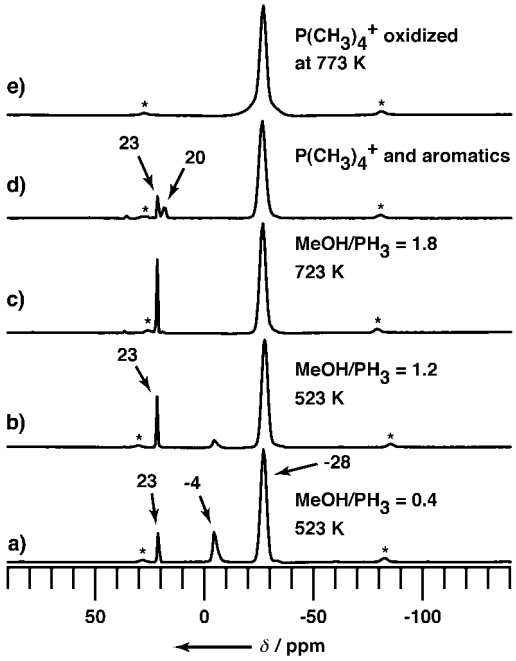

Figure 1. Examples of ^{31}P MAS-NMR spectra showing functionalization of the HSAPO-34 nanocages according to Scheme 1. The chemical shift arising from the phosphorus atoms in the HSAPO-34 framework is $\delta = -28$ ppm. In all cases PH_3 and methanol was passed over the catalyst bed for 10 min. The PH_3 flow rate was 14 sccm except for the sample in c) where 32 sccm was used. Methanol/PH_3 mole ratios are shown where important. a) With a limited amount of methanol, the major product in the nanocages was $P(CH_3)_3$, which was protonated by the Brønsted acid sites ($\delta = -4$ ppm). b) When methanol was in excess, $P(CH_3)_4^+$ (23 ppm) formed in most nanocages. c) With forcing conditions, $P(CH_3)_4^+$ formed in every cage. d) $P(CH_3)_4^+$ yields signals at both $\delta = 23$ ppm and 20 ppm when approximately half of the nanocages also contain aromatic compounds synthesized from methanol. e) If $P(CH_3)_4^+$ is formed in the nanocages and the catalyst is heated to high temperatures in air, a phosphate species forms, as indicated by the broad signal near that of the framework. ⋆ denotes spinning sidebands.

[*] Prof. J. F. Haw, W. Song
Loker Hydrocarbon Research Institute and
Department of Chemistry
University of Southern California
Los Angeles, CA 90089-1661 (USA)
Fax: (+1) 213-740-0930
E-mail: jhaw@usc.edu

[**] This work was supported by the National Science Foundation (CHE-0205939) and (CHE-9996109), and the U.S. Department of Energy (DOE) Office of Basic Energy Sciences (BES; Grant Nos. DE-FG03-93ER14354 and DE-FG03-99ER14956).

  0044-8249/03/11508-0920 $ 20.00+.50/0

$P(CH_3)_4^+$ ion in every nanocage by increasing the flow of PH_3 and methanol. Evidence for this includes the expected 5:1 ratio[8] for the integrals of the ^{31}P resonance signals of the phosphorus atoms of the framework to those of the cation. Figure 1d shows a ^{31}P NMR spectrum of SAPO-34 containing both $P(CH_3)_4^+$ ions and methylbenzene derivatives. Note that with aromatic species present there are two $P(CH_3)_4^+$ resonance signals, one as before at $\delta = 23$ ppm, and one at $\delta = 20$ ppm. We speculate that the signal at $\delta = 20$ ppm arises from $P(CH_3)_4^+$ ions situated in cages with an aromatic ring.

When $P(CH_3)_4^+$ in SAPO-34 was heated to 773 K, it decomposed to an inorganic phosphate species with a chemical shift similar to that of the framework phosphorus. Evidence for this species is visible as a broad feature at the base of the resonance signal at $\delta = -28$ ppm (Figure 1e). An identical ^{31}P signal was observed when we used the same chemistry to functionalize cages in aluminosilicate zeolites (results not shown).

The presence of this phosphate species in our functionalized HSAPO-34 catalyst improves the ethylene selectivity. Figure 2 shows the GC traces from the product streams of reactors converting methanol under steady-state conditions (weight-hourly space velocity, WHSV = 8 h^{-1} at 723 K) by using either standard HSAPO-34 or functionalized materials. For HSAPO-34 without PH_3 treatment, methanol conversion was 100% and ethylene selectivity was 37% (Figure 2a). Conversely, with one $P(CH_3)_4^+$ ion per cage and all acid sites consumed by phosphonium cation formation, conversion was near zero (Figure 2b). Calcination of this sample in the reactor to form a material with a phosphate species in every cage produced a catalyst with greatly improved ethylene selectivity (46%) but reduced activity (Figure 2c). When we prepared a material with a phosphate species in approximately a half of all cages, we achieved 95% conversion and retained an impressive ethylene selectivity of 44% (Figure 2d).

The results shown in Figure 1 and 2 are representative and reproducible. The functionalized catalysts deactivated at the same rate as standard catalysts. The ^{13}C NMR spectra showed, as before,[3] that deactivation occurred through the formation of aromatic species in nanocages well beyond the degree required for an active catalyst. The ^{31}P NMR spectrum of the deactivated catalyst showed that there was no loss of phosphate. Furthermore, we found that the catalyst containing the phosphate species could be reactivated by burning the sample to remove hydrocarbons in the cages. In this way the catalyst regained the activity and selectivity of a freshly prepared sample.

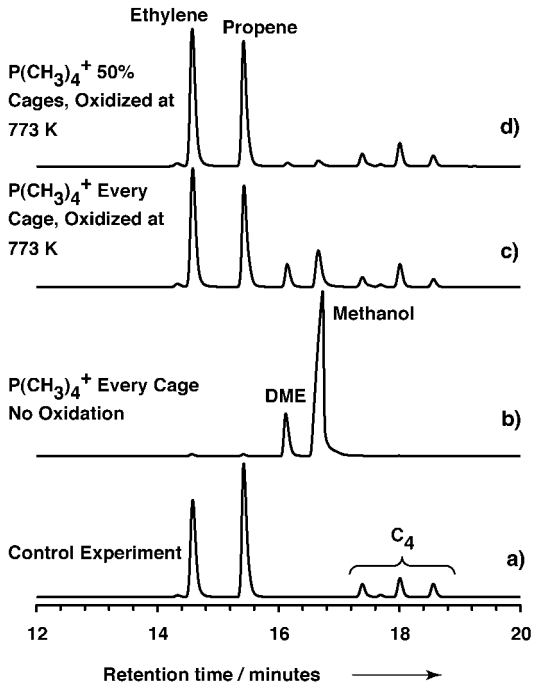

Figure 2. Examples of GC (flame ionization) analyses of the product gases in MTO conversion on catalysts functionalized by introducing phosphorus species into the nanocages. All experiments were performed at 723 K with a methanol WHSV of 8 h^{-1}. a) Control experiment on standard HSAPO-34, 100% conversion, ethylene selectivity 37%. b) Modified catalysts, $P(CH_3)_4^+$ ions in all nanocages, 0% conversion. c) Modified catalyst, phosphate species formed in every nanocage by aerial oxidation (773 K) of the $P(CH_3)_4^+$ ions, 50% conversion, ethylene selectivity 46%. d) Modified catalyst, phosphate formed in 50% of all nanocages by aerial oxidation (773 K) of the $P(CH_3)_4^+$ ions, 95% conversion, ethylene selectivity 44%. Note that the catalyst in this case has nearly the same activity as the standard catalyst, but significantly higher ethylene selectivity. DME = dimethyl ether.

Experimental Section

Functionalized catalyst samples were prepared for NMR studies by thermally quenching the reactor and then transferring the contents to MAS-NMR sample rotors as described previously.[9] The 121 MHz ^{31}P Bloch decay MAS-NMR spectra were acquired on a Chemagnetics CMX-300 spectrometer by using 400 scans, 90° flips, and 10 s delays. For product analysis, gas samples from MTO reactors were collected and introduced into a Hewlett-Packard Model 6890 gas chromatograph by means of a Valco valve. Standard response factors were used to correct the flame ionization response to percent composition.

Received: September 9, 2002 [Z50121]

[1] M. Stöcker, *Microporous Mesoporous Mater.* **1999**, *29*, 3–48.
[2] HSAPO-34 was prepared according to: B. M. Lok, C. A. Messina, R. L. Patton, R. T. Gajek, T. R. Cannan, E. M. Flanigen, US Patent 4,440,871 **1984**. XRD showed a pure crystalline phase with the CHA structure. The product was calcined at 873 K for 10 h to remove the template agent and pressed into 10–20 mesh pellets.
[3] a) W. Song, J. F. Haw, J. B. Nicholas, K. Heneghan, *J. Am. Chem. Soc.* **2000**, *122*, 10726–10727; b) W. Song, H. Fu, J. F. Haw, *J. Am. Chem. Soc.* **2001**, *123*, 4749–4754; other workers have come to similar conclusions, for example, see: c) B. Arstad, S. Kolboe, *J. Am. Chem. Soc.* **2001**, *123*, 8137–8138.
[4] a) W. W. Kaeding, S. A. Butter, US Patent 3,911,041 **1975**; b) H.-N. Sun, US Patent 5,925,586 **1999**.
[5] Air oxidation of catalysts containing $P(CH_3)_3$ gave partial conversion to $OP(CH_3)_3$, which had a ^{31}P chemical shift of $\delta =$ 39 ppm in SAPO-34 (spectra not shown).
[6] The $P(CH_3)_4^+$ ion has been synthesized on the surface of sulfated zirconia catalyst by the disproportionation of $P(CH_3)_3$. J. F. Haw, J. Zhang, K. Shimizu, T. N. Venkatraman, D.-P. Luigi, W. Song, D. H. Barich, J. B. Nicholas, *J. Am. Chem. Soc.* **2000**, *122*, 12561–12570.

  0044-8249/03/11508-0921 $ 20.00+.50/0

[7] W. P. Rothwell, W. Shen, J. H. Lunsford, *J. Am. Chem. Soc.* **1984**, *106*, 2452 – 2453.
[8] Each unit cell of CHA contains 36 T sites and three cages. The HSAPO-34 used has one Si, five P, and six Al atoms per cage.
[9] J. F. Haw, P. W. Goguen, T. Xu, T. W. Skloss, W. Song, Z. Wang, *Angew. Chem.* **1998**, *110*, 993 – 995; *Angew. Chem. Int. Ed.* **1998**, *37*, 948 – 949.

Surface Effects from Nanostructure

Structural Color and the Lotus Effect**

*Zhong-Ze Gu, Hiroshi Uetsuka, Kazuyuki Takahashi, Rie Nakajima, Hiroshi Onishi, Akira Fujishima, and Osamu Sato**

The study of biological microstructure is one of the most important research areas in biomimicry.[1–3] Microstructure plays many important roles in living things.[2,3] For example, the charming blue color of the *Morpho sulkowskyi* butterfly originates from light diffraction and scattering, which results from the ordered microstructure of its scales. This form of color is usually known as structural color, which is utilized by animals both for protection and as a warning. Today, the study of structural color has been extended from biology to optics.[4–6] As well as affecting coloration, microstructure also plays an important role in self-cleaning.[2,7] For the butterfly, the specific nanostructure enhances the hydrophobicity of its wings, which allows droplets of water to be dispersed more easily. During this process, dust particles on the surface of the wings are removed. This phenomenon is known as the "lotus effect", which is not only very useful for natural species, but also for materials applications, such as for decoration where a natural force might be used to clean a surface. It would be interesting to discover whether it is possible to design a material that incorporates both structural color and the lotus effect, thus mimicking the wings of a butterfly. Such a material should be of great biological and technological importance. In this paper, we will show one approach to fabricating such a biomimetic decorative material by taking advantage of a nanostructured inverse opal surface.

Inverse opal is a solid material that consists of a three-dimensional network.[6,8–10] Ordered monodisperse air spheres throughout the network contribute to an optical stop band, the position of which can be tuned by careful control of the periodicity of the air spheres. Colors can be observed by the naked eye when the stop band falls in the visible region. As a consequence of its unique optical properties, inverse opal has been regarded as a new-generation decorative material, in addition to its application as a photonic crystalline material.[6,11] Recently, we realized that inverse opal might also be incorporated into the design of a hydrophobic material. The solid material network of inverse opal contributes a rough surface composed of well-ordered meshes. According to the Cassie–Baxter law, the intrinsic wettability of the solid material can be greatly reduced.[12] Such a decorative material, which exhibits both structural color and the lotus effect, would be environmentally friendly and energy-efficient.

For practical applications, a convenient method of fabricating a uniform inverse opal film over a large area is required. In addition, the rough inverse opal surface needs to be further optimized to imbue the surface with superhydrophobic character. We describe here the development of a dipping method that can be used to meet these criteria, and which can derive uniform inverse opal films with a nanostructured surface. The procedure for the fabrication is as follows: First, submicron-sized monodisperse polystyrene spheres and nanosized particles were ultrasonically dispersed into deionised water. A glass substrate was then immersed into the solution and withdrawn at a constant speed. It is known that a mixture of spheres with different sizes cannot be used to fabricate colloidal crystals with long-range structural order by such a deposition method,[13–15] as phase separation occurs, or an amorphous structure is formed. In our experiment, we found that this conclusion is only partially correct. A structure with long-range order can be derived when the ratio of the diameters of the spheres falls into a particular regime. Figure 1a shows an image of a structure composed of monodisperse spheres, while Figure 1b–d displays three images of structures composed of spheres of two sizes, with diameter ratios of 0.94, 0.34, and 0.07, respectively. The structure formed by the spheres of varying size depends on the diameter ratio. A structure with long-range order can be observed in films composed of monodisperse spheres, however, such order is absent in films composed of spheres of two sizes, where the diameter ratio is larger than 0.15. Usually, the particles form a structure with discernible separation when the ratio between the two types of sphere is larger than 0.5 (Figure 1b), while the domains formed by different types of particles are separated when the ratio is smaller than this value (Figure 1c). When the diameter ratio between the

[*] Dr. O. Sato, Prof. Dr. Z.-Z. Gu, Dr. H. Uetsuka, K. Takahashi, R. Nakajima, Dr. H. Onishi
Kanagawa Academy of Science and Technology
KSP Bldg. East 412, 3-2-1 Sakado, Takatsu-ku, Kawasaki-shi, Kanagawa 213-0012 (Japan)
Fax: (+81) 44-819-2070
E-mail: sato@fchem.chem.t.u-tokyo.ac.jp
Prof. Dr. Z.-Z. Gu
National Laboratory of Molecular and Biomolecular Electronics
Southeast University
Nanjing 210096 (China)
Prof. Dr. A. Fujishima
Department of Applied Chemistry
School of Engineering, The University of Tokyo
7-3-1 Hongo Bunkyo-ku, Tokyo 113-8565 (Japan)

[**] This work was partially supported by a Grant-in-Aid for Scientific Research on Priority Areas (417) from the Ministry of Education, Culture, Sports, Science and Technology (MEXT) of the Japanese Government. Z.-Z.G. also thanks the Research Foundation (60228002) of the National Nature Science Foundation of China.

  0044-8249/03/11508-0922 $ 20.00+.50/0